Sensing-Assisted Secure Uplink Communications with Full-Duplex Base Station

Xinyi Wang, *Graduate Student Member, IEEE*, Zesong Fei, *Senior Member, IEEE*,
J. Andrew Zhang, *Senior Member, IEEE*, and Jingxuan Huang

***Abstract*—This letter proposes a sensing-assisted uplink communications framework between a single-antenna user and a full-duplex (FD) base station (BS) against an aerial eavesdropper (AE). To protect the information from being overheard, the BS transmits radar signals to localize and jam AE while receiving uplink signals. The radar signal transmission is divided into detection phase and tracking phase. In detection phase, the BS synthesizes a wide beam to localize the AE under the secrecy rate constraint; while in tracking phase, the BS maximizes the signal-to-interference-plus-noise ratio (SINR) of its received signals under the AE's SINR constraint while guaranteeing a predefined radar echo signal signal-to-noise ratio (SNR) level. To deal with the self interference, we jointly optimize the radar waveform and receive beamforming vector. An alternating optimization algorithm and a successive convex approximation (SCA) based algorithm are proposed to solve the two formulated problems, respectively. Simulation results verify the effectiveness of the proposed algorithms. They also show that the secrecy rate can be significantly improved with the assistance of BS sensing.**

Keywords: Sensing-assisted secure communications, aerial eavesdropper, secrecy rate, beampattern design.

I. Introduction

Due to the broadcast nature of wireless communications, the transmitted signals are accessible to both legitimate users and eavesdroppers, thus making wireless transmissions vulnerable to eavesdropping. Physical-layer security (PLS) has been viewed as a promising technique to enable secure information transmission from an information-theoretic perspective [1].

The basic idea of PLS is to exploit the characteristics of the wireless channel, including noise, fading, interference, etc., such that the performance difference between the link of the legitimate receiver and that of the eavesdropper can be significantly enlarged. In this sense, compared with downlink communications, where multi-antenna technique can be employed at the base station (BS) to simultaneously transmit information signals and artificial noise, uplink communciations may be more vulnerable, especially for single-antenna users. According to [2], the security threat becomes even severer when unauthorized unmanned aerial vehicles (UAVs) are deployed as aerial eavesdroppers (AEs). Although the jamming technique can deteriorate the received signals at the eavesdropper, this requires the jammer to know the channels among transmitter, receiver, eavesdropper, and itself, which is generally impractical. Fortunately, the development of full-duplex (FD) techniques [3] has enabled the receiver to simultaneously receive information signals from the transmitter and transmit jamming signals to interfere eavesdroppers [4]–[7]. In [4], the authors designed the optimal jamming covariance matrix to mitigate the self interference and maximize the secrecy rate. In [5], the authors extended the beamforming design from single-input multi-output (SIMO) transmission to multi-input multi-output (MIMO) transmission. As a step further, in [6], a cooperative transmission scenario with a relay is considered. Furthermore, in [7], the effect of the FD transceiver's in-phase and quadrature imbalance was analysed.

Although the FD technique at BS avoids the acquisition of jammer-user channel state information (CSI), the CSI between the BS and AE still needs to be estimated. To this end, it was stated in [8] that with the aid of sensing, the BS is able to monitor unauthorized UAVs and acquire CSI by exploiting the line-of-sight (LOS) communications link, thus enabling the jamming process. There have been some works [9], [10] investigating the sensing ability of BS in uplink communications. In [9], the authors considered the case where the BS simultaneously detects the target and conducts communications, where joint outer bounds were derived to characterize estimation rate and communication rate. In [10], the authors considered an orthogonal frequency-division multiplexing (OFDM) system, where both radar and communication systems share overlapping subcarriers. However, the secrecy performance gain introduced by the sensing ability has not been demonstrated in the existing literatures. In addition, existing works, which consider dual-functional radar-communications and PLS [11], [12], mainly focus on the downlink cases.

In this letter, we investigate a sensing-aided secure uplink communication system from a single-antenna user to an FD BS. To protect the information from being overheard by an AE, while receiving the uplink signals, the BS also transmits radar signals to localize and jam the AE. The main contributions can be summarized as follows.

- We propose a method to exploit the sensing ability of the receiver to obtain partial CSI of AE and jam AE accordingly. This method can enable us to significantly improve the secrecy performance of communications, while achieving high spectral efficiency;
- We propose a two-phase solution for implementing the method, including detection and tracking, based on alternating optimization and successive convex approximation (SCA) techniques. This solution provides a practical and effective way for joint receive beamforming vector and transmit waveform design for BS.
- Simulation results show that with the aid of sensing ability, the secrecy performance can be significantly improved compared with the conventional full-duplex receiver [6].

This work was supported in part by the National Natural Science Foundation of China under Grant U20B2039, in part by National Natural Science Foundation of China under 61871032, and in part by the Australian Research Council under grant No. DP210101411. *(Corresponding author: Zesong Fei.)*

Xinyi Wang, Zesong Fei and Jingxuan Huang are with the School of Information and Electronics, Beijing Institute of Technology, Beijing 100081, China. E-mail:bit_wangxy@163.com, feizesong@bit.edu.cn, jxhbit@gmail.com.

J. Andrew Zhang is with the School of Electrical and Data Engineering, University of Technology Sydney, NSW, Australia 2007. E-mail:Andrew.Zhang@uts.edu.au

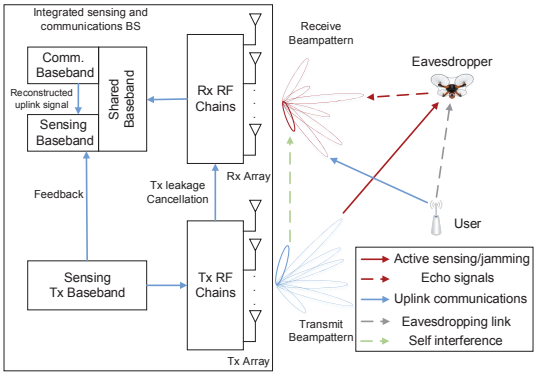

Fig. 1: An illustration of the secure uplink communication system against the aerial eavesdropper.

Notations: $a, \mathbf{a}, \mathbf{A}$ denote complex scalar value, vector, matrix, respectively; $\mathbb{C}$ denotes the set of complex numbers; $[\cdot]^*$, $[\cdot]^T$, and $[\cdot]^H$ denote the conjugate, transpose and conjugate-transpose operations, respectively.

II. System Model

We consider a secure uplink communication system consisting of one FD BS, one single-antenna user, and one single-antenna aerial eavesdropper (AE) which circles over the user, as shown in Fig. 1. We assume that the AE in the air is in the line of sight (LOS) of the BS [2], and the user is in the more general non line of sight (NLOS), whose channel model includes the LOS one as a special case. We assume the BS is equipped with half-wavelength spaced uniform linear array (ULA), in which N_R antennas are used for reception and N_T antennas are used for transmission [6]. The radiation pattern of each antenna element is assumed to be omni-directional. When receiving the uplink signals from the user, the BS also transmits radar signals, which are used to jam the detected unauthorized AE while their echo signals are used to locate the aerial vehicle. Upon receiving the echo signals and the uplink communication signals, the BS firstly performs combining and demodulates the uplink signals. It then extracts the echo signals from the received signals by performing interference cancellation. In this way, it has been reported in [10] that the radar echo and communication signals can be successfully separated. Therefore, in this paper, at the receiver side, we focus on the communication aspect.

Let $\mathbf{h}_{ub} \in \mathbb{C}^{N_R \times 1}$, $\mathbf{h}_{be} \in \mathbb{C}^{N_T \times 1}$, and $h_{ue} \in \mathbb{C}^{1\times 1}$ denote the channels from user to BS, from BS to AE, and from user to AE, respectively. Here, $\mathbf{h}_{ub}$ consists of both large-scale path loss and small-scale Rayleigh fading and can be expressed as

$$\mathbf{h}_{ub} = \sqrt{\rho_0 d_{u,b}^{-2}}\tilde{\mathbf{h}}_{ub}, \tag{1}$$

where ρ denotes the channel power at the reference distance $d_0 = 1$ m, $d_{u,b}$ denotes the distance from the user to BS, $\tilde{\mathbf{h}}_{ub}$ follows the standard complex Gaussian distribution. Comparatively, $\mathbf{h}_{be}$ and h_{ue} consist of large-scale path loss and small-scale Rician fading due to the existence of the LOS path. According to [13], $\mathbf{h}_{be}$ and h_{ue} can be are expressed as

$$\begin{aligned}\mathbf{h}_{be} &= \sqrt{\rho_0 d_{b,e}^{-2}}\left(\sqrt{\frac{K_r}{K_r+1}}\mathbf{a}(\theta_0) + \sqrt{\frac{1}{K_r+1}}\tilde{\mathbf{h}}_{be}\right),\\ h_{ue} &= \sqrt{\rho_0 d_{u,e}^{-2}}\left(\sqrt{\frac{K_r}{K_r+1}}\bar{h}_{ue,los} + \sqrt{\frac{1}{K_r+1}}\tilde{h}_{ue}\right),\end{aligned} \tag{2}$$

where $d_{b,e}$ and $d_{u,e}$ denote the distance from BS to AE, and distance from user to AE, respectively, θ_0 denotes the angle of departure (AoD) of AE, $\mathbf{a}(\theta_0) = [1, e^{j2\pi\delta\sin(\theta_0)}, \cdots, e^{j2\pi(N-1)\delta\sin(\theta_0)}]^T$ is the antenna steering vector with δ denoting the normalized interval between adjacent antennas, $\bar{h}_{ue}$ denotes the deterministic LOS channel component with $|\bar{h}_{ue,los}| = 1$, $\tilde{\mathbf{h}}_{be}$ and $\tilde{h}_{ue}$ follow the standard complex Gaussian distribution, and K_r denotes the Rician factor.

Let $\mathbf{H}_{SI} \in \mathbb{C}^{N_R \times N_T}$ denote the self interference (SI) channel from the Tx array to Rx array. According to [16], $\mathbf{H}_{SI}$ can be expressed as

$$\mathbf{H}_{SI} = \eta\tilde{\mathbf{H}}_{SI}, \tag{3}$$

where η represents the equivalent channel gain of residual SI, and $\tilde{\mathbf{H}}_{SI}$ follows the standard complex Gaussian distribution.

The signal received by the BS can be expressed as

$$\mathbf{y}_b = \mathbf{h}_{ub}s + \underbrace{\mathbf{H}_{SI}\mathbf{x}}_{\text{SI}} + \underbrace{\alpha\mathbf{a}^*(\theta_0)\mathbf{a}^H(\theta_0)\mathbf{x}}_{\text{Echo signal}} + \mathbf{n}_b, \tag{4}$$

where s is the uplink signal transmitted by the user, $\mathbf{x}$ represents the radar signal transmitted by BS, with $\mathbf{Q}$ denoting the covariance matrix of $\mathbf{x}$, $\mathbf{n}_b \sim \mathcal{CN}(\mathbf{0}, \sigma_b^2\mathbf{I})$ includes the noise and clutter at BS [10], and α consists of the effects of path loss and radar cross-section (RCS), and can be expressed as [17]

$$\alpha = \sqrt{\rho_0/d_{b,e}^2 \times \xi/d_{b,e}^2}, \tag{5}$$

where ξ represents the RCS, and $d_{b,e}$ denotes the distance from the BS to AE.

By employing a linear receiver, $\mathbf{w}_r$, to the received signals, the SINR of the uplink signals at BS can be expressed as

$$\gamma_b = \frac{P_u\mathbf{w}_r^H\mathbf{h}_{ub}\mathbf{h}_{ub}^H\mathbf{w}_r}{\mathbb{E}\left\{|\mathbf{w}_r^H\bar{\mathbf{H}}_{SI}\mathbf{x}|^2\right\} + \sigma_b^2} = \frac{P_u\mathbf{w}_r^H\mathbf{h}_{ub}\mathbf{h}_{ub}^H\mathbf{w}_r}{\mathbf{w}_r^H\bar{\mathbf{H}}_{SI}\mathbf{Q}\bar{\mathbf{H}}_{SI}^H\mathbf{w}_r + \sigma_b^2}, \tag{6}$$

where P_u denotes user's transmit power, $\bar{\mathbf{H}}_{SI} = \mathbf{H}_{SI} + \alpha\mathbf{a}^*(\theta_0)\mathbf{a}^H(\theta_0)$ denotes the generalized self-interference which is comprised of both self-interference and echo signal.

Similarly, the received signal at AE can be expressed as

$$y_e = h_{ue}s + \mathbf{h}_{be}^H\mathbf{x} + n_e, \tag{7}$$

where n_e denotes the noise at AE with the power of σ_e^2. Since the AE is a non-cooperative target, it is impractical to obtain the perfect CSI of the AE. Therefore, we assume that the BS can only make use of the estimated direction of AE. The corresponding estimated SINR of the signals received by AE and secrecy rate can be respectively expressed as

$$\tilde{\gamma}_e(\theta) = \frac{P_u|\bar{h}_{ue}|^2}{\mathbb{E}[\bar{\mathbf{h}}_{be}^H\mathbf{x}\mathbf{x}^H\bar{\mathbf{h}}_{be}] + \sigma_e^2} = \frac{P_u|\bar{h}_{ue}|^2}{\bar{\mathbf{h}}_{be}^H\mathbf{Q}\bar{\mathbf{h}}_{be} + \sigma_e^2}, \tag{8}$$

$$\tilde{R}_s = [\log_2(1+\gamma_b) - \log_2(1+\tilde{\gamma}_e(\theta))]^+, \tag{9}$$

where $\bar{\mathbf{h}}_{be} = \sqrt{\frac{\rho_0}{d_{b,e}^2}\cdot\frac{K_r}{K_r+1}}\mathbf{a}(\theta)$, and $\bar{h}_{ue} = \sqrt{\frac{\rho_0}{d_{u,e}^2}\cdot\frac{K_r}{K_r+1}}$. Note that the location of user is known to the BS; thus, the distance between user and AE can be estimated by BS based on the estimated location of AE.

As for radar sensing, the transmit beampattern is given as

$$P_d(\theta) = \mathbf{a}^H(\theta)\mathbb{E}\{\mathbf{x}\mathbf{x}^H\}\mathbf{a}(\theta) = \mathbf{a}^H(\theta)\mathbf{Q}\mathbf{a}(\theta). \tag{10}$$

The power of echo signals from the direction θ_0 is given as $P_{echo} = \|\mathbf{A}(\theta_0)\mathbf{x}\|^2$, where $\mathbf{A}(\theta_0) = \alpha \mathbf{a}^*(\theta_0)\mathbf{a}^H(\theta_0)$. Note that after the demodulated uplink signals are subtracted from the received signal, the self-interference cancellation technique in conventional radar systems can be employed to mitigate the impact of the self-interference. Therefore, the SNR of the echo signals is adopted as the performance metric for radar sensing.

III. Problem Formulation

In practice, the AE's direction is unknown to the BS. Instead, the BS has to sense the area of interest to localize the AE. Therefore, we consider a two-phase scheme where the BS firstly synthesizes a wide beam to localize the AE, and then optimize the beamforming vector to maximize the received SINR at the BS under the constraint of AE's SINR while tracking the AE. Note that both jamming performance and DOA estimation accuracy depend on the LOS propagation. Therefore, the criteria of waveform design for sensing and jamming are inherently the same. However, the self-interference constraint would constrain the degrees of freedom in waveform design. In this sense, there exists trade-off between the sensing and communication functionalities.

A. Waveform Design in Detection Phase

For detecting the AE, we consider the case that the BS intends to search the space with angles within $\Omega = [\theta_0 - \Delta\theta/2, \theta_0 + \Delta\theta/2]$. To this end, we aim to synthesize a wide radar beam to provide robust and secure communications by jointly designing the radar transmit covariance matrix $\mathbf{Q}$ and receive beamforming vector $\mathbf{w}_r$. Following the principle in [12], we aim to maximize the difference between mainlobe and sidelobe, while keeping a constant power in the angle interval Ω, which can be formulated as follows. Note that although the radar signal is used to sense and jam the AE, it will also affect the self-interference. Therefore, the radar signal needs to be carefully designed.

$$\max_{\mathbf{Q},\mathbf{w}_r} \min_{\theta_m \in \Phi} \mathbf{a}^H(\theta_0)\mathbf{Q}\mathbf{a}(\theta_0) - \mathbf{a}^H(\theta_m)\mathbf{Q}\mathbf{a}(\theta_m) \tag{11}$$

$$s.t. \quad \log_2(1+\gamma_b) - \log_2(1+\tilde{\gamma}_e(\theta_k)) \geqslant r_s, \forall \theta_k \in \Omega \tag{11a}$$

$$\mathbf{a}(\theta_k)\mathbf{Q}\mathbf{a}(\theta_k) \leqslant (1+\lambda)\mathbf{a}(\theta_0)\mathbf{Q}\mathbf{a}(\theta_0), \forall \theta_k \in \Omega \tag{11b}$$

$$(1-\lambda)\mathbf{a}(\theta_0)\mathbf{Q}\mathbf{a}(\theta_0) \leqslant \mathbf{a}(\theta_k)\mathbf{Q}\mathbf{a}(\theta_k), \forall \theta_k \in \Omega \tag{11c}$$

$$\mathrm{Tr}(\mathbf{Q}) \leqslant P_0, \ \mathbf{Q} \succeq 0, \tag{11d}$$

$$\|\mathbf{w}_r\| = 1, \tag{11e}$$

where Φ denotes the sidelobe region of interest. The constraint (11a) sets a low bound r_s for the secrecy rate, while the constraints (11b) and (11c) guarantees that the mainlobe of the optimized waveform maintains a nearly constant power with $\lambda < 0.05$.

B. Waveform Design in Tracking Phase

After the detection phase, the BS has AE's angular information. It then transmit sensing signals to jam AE and tracks AE based on the echo signals. In this phase, we focus on maximizing the SINR of the received uplink signals under the constraint of the AE's SINR, while guaranteeing a predefined radar echo signal's SNR. Although velocity estimation is also important in tracking AE, its accuracy depends on echo signal's SNR, and we refer readers to [14] for explicit velocity estimation of UAV. To reduce the implementation complexity, we jointly design the radar signal $\mathbf{x}$ and receive beamforming vector $\mathbf{w}_r$. The problem can be formulated as follows.

$$\max_{\mathbf{x},\mathbf{w}_r} \gamma_b \tag{12}$$

$$s.t. \ \tilde{\gamma}_e(\theta_0) \leqslant \gamma_{th}, \tag{12a}$$

$$\mathbf{x}^H\mathbf{A}^H(\theta_0)\mathbf{A}(\theta_0)\mathbf{x} \geqslant \gamma_{echo}\sigma_b^2, \tag{12b}$$

$$\|\mathbf{x}\|^2 \leqslant P_0, \tag{12c}$$

$$\|\mathbf{w}_r\| = 1, \tag{12d}$$

where γ_{th} is a predefined threshold of the AE's SINR, γ_{echo} is a predefined threshold of the echo signal's SNR, and θ_0 is estimated and updated by the BS with the motion of AE.

IV. Proposed Algorithms

A. Algorithm for Solving Problem (11)

To address the coupled variables in problem (11), we propose an alternating optimization algorithm for jointly designing $\mathbf{w}_r$ and $\mathbf{Q}$.

1) Optimization of $\mathbf{w}_r$ for Given $\mathbf{Q}$: For any given $\mathbf{Q}$, we observe that only γ_b in the constraint (12a) depends on $\mathbf{w}_r$. To maximize the degrees of freedom (DoFs) reserved for the design of $\mathbf{Q}$, we propose to optimize $\mathbf{w}_r$ by maximizing γ_b. In this way, $\mathbf{w}_r$ can be expressed as the solution to the following problem.

$$\max_{\|\mathbf{w}_r\|=1} \frac{\mathbf{w}_r^H\mathbf{H}_{ub}\mathbf{w}_r}{\mathbf{w}_r^H\mathbf{C}\mathbf{w}_r}, \tag{13}$$

where $\mathbf{C} = \bar{\mathbf{H}}_{SI}\mathbf{Q}\bar{\mathbf{H}}_{SI}^H + \sigma_b^2\mathbf{I}$, and $\mathbf{H}_{ub} = \mathbf{h}_{ub}\mathbf{h}_{ub}^H$. Therefore, the optimum $\mathbf{w}_r$ can be derived as

$$\mathbf{w}_r = \frac{\mathbf{C}^{-1}\mathbf{h}_{ub}}{\|\mathbf{C}^{-1}\mathbf{h}_{ub}\|} \tag{14}$$

2) Optimization of $\mathbf{Q}$ for Given $\mathbf{w}_r$: For any given $\mathbf{w}_r$, we first recast the problem (11) as

$$\max_{t,\mathbf{Q}} \ t \tag{15}$$

$$s.t. \ \ \mathbf{a}^H(\theta_0)\mathbf{Q}\mathbf{a}(\theta_0) - \mathbf{a}^H(\theta_m)\mathbf{Q}\mathbf{a}(\theta_m) \geqslant t, \forall \theta_m \in \Phi, \tag{15a}$$

$$(11a) \sim (11e).$$

We propose to solve the problem (15) by reformulating it into two sub-problems. First, it can be shown that there always exists an SINR constraint γ_1 such that the problem (15) has the same optimal solution to the following problem [15].

$$\max_{t,\mathbf{Q}} \ t \tag{16}$$

$$s.t. \ \ \gamma_b \geqslant \gamma_1, \tag{16a}$$

$$\gamma_e(\theta_k) \leqslant \frac{1+\gamma_1}{2^{r_s}} - 1, \forall \theta_k \in \Omega, \tag{16b}$$

$$(11b) \sim (11e), (15a).$$

which is convex. Let $g(\gamma_1)$ denote the optimal value of the objective function in problem (16) associated with γ_1. We can then obtain the optimal value of problem (15) by solving the following problem.

$$\max_{\gamma_1 > 0} \ g(\gamma_1). \tag{17}$$

Let γ_1^* denote the optimal solution to problem (17). With $\gamma_1 = \gamma_1^*$, it can be readily seen that the problem (15) and problem (16) have the same optimal solution [15]. Therefore, the problem (15) can be solved via the following two-loop

optimization strategy: in the outer loop, the optimal γ_1 for problem (17) is obtained via one-dimension search over $\gamma_1 > 0$; while in the inner loop, for any given γ_1, $g(\gamma_1)$ is obtained by solving problem (16). The solution is optimal to (15) as the optimal value of (15) is the same as that of (17) [15]. The computational complexity of obtaining an ϵ-optimal solution for optimizing $\mathbf{Q}$ in each iteration is $\mathcal{O}\left(N^{6.5}\ln(1/\epsilon)\right)$ [12].

Algorithm 1 Overall Alternating Optimization Algorithm for Solving Problem (11)

1: Initialize $\mathbf{Q}^{[0]}$ and $\mathbf{w}_r^{[0]}$ as feasible solutions for problem (11), set $t = 0$.
2: **repeat**
3: For given $\mathbf{Q}^{[t]}$, update $\mathbf{w}_r^{[t+1]}$ as (14).
4: Perform one-dimension search to obtain optimal γ_1^* for the problem (17) and update $\mathbf{Q}^{[t+1]}$.
5: For each given γ_1, solve the problem (16).
6: Update $t = t + 1$.
7: **until** the value of objective function (11) converges or the maximum iteration is reached.

3) Overall Algorithm for solving the problem (11): The overall alternating optimization algorithm is summarized in Algorithm 1. Note that the objective function is monotonically non-decreasing in each iteration. Therefore, Algorithm 1 is guaranteed to converge. According to [18], to synthesize a wide mainlobe, the obtained $\mathbf{Q}$ is full-rank in general. For detailed implementation of generating time-variant beamformer based on $\mathbf{Q}$, we refer readers to [18].

B. Algorithm for Solving Problem (12)

In this section, we propose an iterative algorithm to solve the problem (12). By substituting (14) into (6) and utilizing the Sherman-Morrison formula [6], γ_b can be written as

$$\begin{aligned}\gamma_b &= P_u \mathbf{h}_{ub}^H (\bar{\mathbf{H}}_{SI}\mathbf{x}\mathbf{x}^H\bar{\mathbf{H}}_{SI}^H + \mathbf{B})^{-1}\mathbf{h}_{ub} \\ &= P_u\left(\mathbf{h}_{ub}^H\mathbf{B}^{-1}\mathbf{h}_{ub} - \frac{|\mathbf{h}_{ub}^H\mathbf{B}^{-1}\bar{\mathbf{H}}_{SI}\mathbf{x}|^2}{1+\mathbf{x}^H\bar{\mathbf{H}}_{SI}^H\mathbf{B}^{-1}\bar{\mathbf{H}}_{SI}\mathbf{x}}\right),\end{aligned}$$

where $\mathbf{B} = \sigma_b^2\mathbf{I}$.

The problem (12) can then be converted to

$$\min_{\mathbf{x}} \ \frac{|\mathbf{h}_{ub}^H\mathbf{B}^{-1}\bar{\mathbf{H}}_{SI}\mathbf{x}|^2}{1+\mathbf{x}^H\bar{\mathbf{H}}_{SI}^H\mathbf{B}^{-1}\bar{\mathbf{H}}_{SI}\mathbf{x}} \tag{18}$$
$$s.t.\ \mathbf{x}^H\bar{\mathbf{h}}_{be}\bar{\mathbf{h}}_{be}^H\mathbf{x} + \sigma_e^2 \geqslant P_u|\bar{\mathbf{h}}_{ue}|^2/\gamma_{th}, \tag{18a}$$
$$(12b), (12c),$$

To deal with the non-convex objective function, the problem (18) is further converted to

$$\min_{\mathbf{x},z,u_1,v_1} \ z \tag{19}$$
$$s.t.\ \mathbf{x}^H\mathbf{D}\mathbf{x} \leqslant u_1^2, \tag{19a}$$
$$1+\mathbf{x}^H\bar{\mathbf{H}}_{SI}^H\mathbf{B}^{-1}\bar{\mathbf{H}}_{SI}\mathbf{x} \geqslant v_1, \tag{19b}$$
$$u_1^2/v_1 \leqslant z, \tag{19c}$$
$$(12b), (12c), (18a)$$

where $\mathbf{D} = \bar{\mathbf{H}}_{SI}^H\mathbf{B}^{-1}\mathbf{h}_{ub}\mathbf{h}_{ub}^H\mathbf{B}^{-1}\bar{\mathbf{H}}_{SI}$. However, the constraints (12b), (18a), (19a), and (19b) are still non-convex. We then apply Taylor series expansion and SCA technique to address them below.

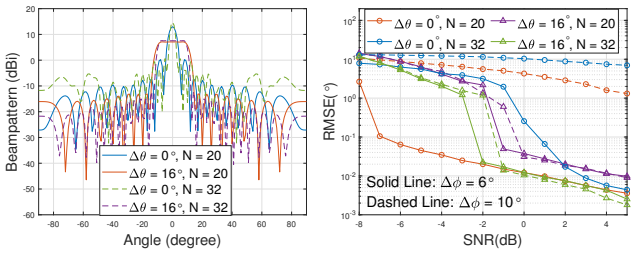

(a) (b)

Fig. 2: (a) Radar beampatterns with different angle intervals of interest. (b) RMSE of the AE's DOA estimation versus echo signal SNR, r_s = 3 bit/s/Hz.

*Transformation of (12*b), (18a), and (19b): By applying the first-order Taylor series expansion around $\tilde{\mathbf{x}}$, (12b), (18a), and (19b) can be respectively relaxed as

$$2\mathrm{Re}\{\tilde{\mathbf{x}}^H\mathbf{A}^H\mathbf{A}\mathbf{x}\} - \tilde{\mathbf{x}}^H\mathbf{A}^H\mathbf{A}\mathbf{x} \geqslant \gamma_{echo}\sigma_b^2, \tag{20}$$
$$2\mathrm{Re}\{\tilde{\mathbf{x}}^H\bar{\mathbf{h}}_{be}\bar{\mathbf{h}}_{be}^H\mathbf{x}\} - \tilde{\mathbf{x}}^H\bar{\mathbf{h}}_{be}\bar{\mathbf{h}}_{be}^H\tilde{\mathbf{x}} \geqslant P_u|\bar{\mathbf{h}}_{ue}|^2/\gamma_{th} - \sigma_e^2, \tag{21}$$
$$2\mathrm{Re}\{\tilde{\mathbf{x}}^H\bar{\mathbf{H}}_{SI}^H\mathbf{B}^{-1}\bar{\mathbf{H}}_{SI}\mathbf{x}\} - \tilde{\mathbf{x}}^H\bar{\mathbf{H}}_{SI}^H\mathbf{B}^{-1}\bar{\mathbf{H}}_{SI}\tilde{\mathbf{x}} \geqslant v_1 - 1. \tag{22}$$

Transformation of (19a): We apply the first-order Taylor series expansion on $\tilde{u}_1$ and linearize (19a) as

$$\mathbf{x}^H\mathbf{D}\mathbf{x} \leqslant 2\tilde{u}_1u_1 - \tilde{u}_1^2. \tag{23}$$

Based on the aforementioned transformations, the problem (19) can be approximated as

$$\min_{\mathbf{x},z,u_1,v_1} \ z \tag{24}$$
$$s.t.\ (12c), (19a), (20), (21), (22), (23)$$

The original problem (12) can be solved via iteratively solving the problem (24). In each iteration, the computational complexity is $\mathcal{O}\left(N^3\ln(1/\epsilon)\right)$.

V. Simulation Results

In this section, we validate the proposed joint transmit covariance matrix and receive beamforming design algorithms via numerical results. We assume the AE circles over the user. Without loss of generality, θ_0 is set as 0°, and the number of antennas for transmitting and receiving signals are set as $N_T = N_R = N$. The noise power σ^2 and ρ_0 are set as -110 dBm and -60 dB, respectively [17]. The transmit power of BS and user are set as 20 dBm and 0 dBm, respectively. The Rician factor is selected as $K_r = 10$, and η is set as -70 dB.

We first investigate the performance of the proposed algorithm for the detection phase. In Fig. 2(a), we show the obtained radar beampatterns with different angle intervals. The secrecy rate constraint is set as $r_s = 3$ bit/s/Hz. As can be seen, the obtained beampattern maintains a constant mainlobe gain in the region of possible target location, and the expansion of mainlobe is at the expense of the reduction of mainlobe gain and the estimation accuracy. To illustrate this trade-off, we show the root mean square error (RMSE) of the direction of arrival (DOA) estimation under different $\Delta\theta$'s in Fig. 2(b). To show the robustness of the mainlobe in detecting the AE, we assume that the AE is randomly located at $[-\Delta\phi/2, \Delta\phi/2]$. It shows that for $\Delta\phi = 6^\circ$, the estimation accuracy is higher with the waveform designed with a smaller $\Delta\theta$, since the mainlobe gain is higher in this region. However, for $\Delta\phi = 10^\circ$, the estimation accuracy under $\Delta\theta = 0^\circ$ degrades severely. This phenomenon demonstrates

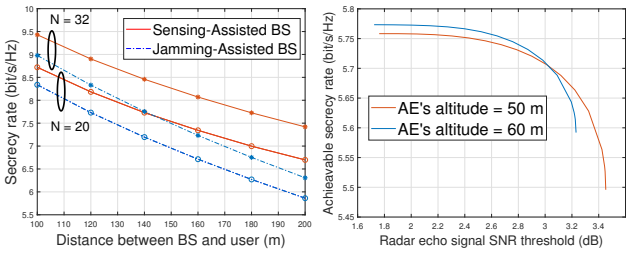

(a) (b)

Fig. 3: (a) Secrecy rate v.s. distance between BS and user, AE's altitude = 40 m. (b) Secrecy rate v.s. echo signal SNR threshold, BS-user distance = 200 m. (γ_{th} = 0.1)

the trade-off between the estimation accuracy and the detection range. Specifically, to support the high-accuracy estimation of a wider DOA, a wider mainlobe is required; while a narrower mainlobe leads to higher estimation accuracy in its mainlobe, thus is more appropriate for estimating the DOA in a narrow range. We also present the performance with $N = 32$. As can be seen, with a larger antenna array, the passband between the mainlobe and sidelobe of the beampattern is narrower. As a result, the DOA estimation performance is less robust to the uncertainty of the AE's direction. On the other hand,when $\Delta\theta \geq \Delta\phi$, the RMSE of the DOA estimation is lower with $N = 32$. This indicates that the aforementioned trade-off is more prominent under a larger antenna number. Note that since partial CSI of AE is constructed based on the estimated DOA, the RMSE of DOA estimation can also reflect the accuracy of the constructed CSI.

We then demonstrate the effectiveness of utilizing the sensing capability of an FD BS in safeguarding the uplink communications. Note that although only the LOS components are used in optimization, the evaluation of secrecy rate is based on the whole CSI, i.e., both LOS and NLOS components are taken into consideration when evaluating the secrecy rate. In Fig. 3(a), we compare the secrecy rate between the sensing-assisted BS and the full-duplex jamming-assisted BS [6] to show the advancement of the BS with sensing ability, where γ_{echo} is set as 1.5 dB. Since the CSI of AE is unavailable due to the absence of sensing ability, we assume the jamming-assisted BS transmits the jamming signals that cause minimum interference to itself. As can be seen, with the distance from BS to user increasing, the secrecy rate decreases due to the increasing path loss. With the aid of radar sensing based CSI estimation, the sensing-assisted BS can achieve significant gain in secrecy rate. Besides, as the antenna number increases, the secrecy rate gain of the sensing-assisted BS also increases. This indicates that the sensing-assisted jamming technique is more effective since partial CSI can be estimated. Also note that the performance gain is even larger with higher AE's altitude, since the partial CSI plays a more important role. In addition, the trade-off between secrecy rate and the echo signal SNR constraint is illustrated in Fig. 3(b). As can be seen, with the increasing requirement of the echo signal SNR, the DoFs of radar waveform are constrained, resulting in increased SI, thus decreasing the secrecy rate. Since the AE may adjust its altitude, we evaluate the secrecy rate under different AE's altitude. With a low SNR threshold of the echo signal, the secrecy rate under higher AE's altitude is higher, since the distance between AE and user is longer. However, when the SNR threshold is higher, the DOF of designing radar signals under higher AE's altitude is more restricted; thus, the secrecy rate performance is poorer than that under lower AE's altitude.

VI. Conclusion

In this letter, we proposed a sensing-assisted secure uplink communication framework between a single-antenna user and an FD BS against an AE. In the detection phase, the BS synthesizes a wide beam to detect the unauthorized AE while guaranteeing secure uplink transmission. An alternating optimization algorithm was proposed to jointly design the transmit waveform and receive filter. Simulation results demonstrate the trade-off between the estimation accuracy and detection range, which is even prominent with a larger antenna array. In the tracking phase, the BS maximizes the SINR of its received signals under the constraints of radar echo signal SNR and AE's SINR via an SCA-based algorithm. Simulation results show that the secrecy rate can be significantly improved compared with the conventional FD BS, since the sensing ability can be exploited to obtain partial CSI of the AE.

References

[1] D. Wang, B. Bai, W. Zhao, and Z. Han, "A survey of optimization approaches for wireless physical layer security," *IEEE Commun. Surveys Tuts.,* vol. 21, no. 2, pp. 1878-1911, Secondquarter 2019.

[2] X. Yuan, Z. Feng, W. Ni, R. P. Liu, J. A. Zhang, and W. Xu, "Secrecy performance of terrestrial radio links under collaborative aerial eavesdropping," *IEEE Trans. Inf. Forensics Security,* vol. 15, pp. 604-619, 2020.

[3] H. Alves, T. Riihonen, and H. A. Suraweera, *Full-Duplex Communications for Future Wireless Networks,* Springer, 2020.

[4] G. Zheng, I. Krikidis, J. Li, A. P. Petropulu, and B. Ottersten, "Improving physical layer secrecy using full-duplex jamming receivers," *IEEE Trans. Signal Process.,* vol. 61, no. 20, pp. 4962-4974, Oct.15, 2013.

[5] Y. Zhou, Z. Z. Xiang, Y. Zhu, and Z. Xue, "Application of full-duplex wireless technique into secure MIMO communication: Achievable secrecy rate based optimization," *IEEE Signal Process. Lett.,* vol. 21, no. 7, pp. 804-808, July 2014.

[6] F. Jafarian, Z. Mobini, and M. Mohammadi, "Secure cooperative network with multi-antenna full-duplex receiver," *IEEE Syst. J.,* vol. 13, no. 3, pp. 2786-2794, Sept. 2019.

[7] L. Samara, R. Hamila, and N. Al-Dhahir, "Secrecy performance of full-duplex jamming and reception under I/Q imbalance," *IEEE Trans. Veh. Technol.,* vol. 70, no. 9, pp. 9560-9565, Sept. 2021.

[8] F. Liu, C. Masouros, A. P. Petropulu, H. Griffiths, and L. Hanzo, "Joint radar and communication design: Applications, state-of-the-art, and the road ahead," *IEEE Trans. Commun.,* vol. 68, no. 6, pp. 3834-3862, June 2020.

[9] C. Li, N. Raymondi, B. Xia, and A. Sabharwal, "Outer bounds for MIMO communicating radars: Three-node uplink," in *2018 52nd Asilomar Conference on Signals, Systems, and Computers, Pacific Grove,* CA, USA, 2018, pp. 934-938.

[10] M. Temiz, E. Alsusa, and L. Danoon, "A receiver architecture for dual-functional massive MIMO OFDM RadCom systems," in *2020 IEEE International Conference on Communications Workshops (ICC Workshops),* Dublin, Ireland, 2020, pp. 1-6.

[11] A. Deligiannis, A. Daniyan, S. Lambotharan, and J. A. Chambers, "Secrecy rate optimizations for MIMO communication radar," *IEEE Trans. Aerosp. Electron. Syst.,* vol. 54, no. 5, pp. 2481-2492, Oct. 2018.

[12] N. Su, F. Liu, and C. Masouros, "Secure radar-communication systems with malicious targets: Integrating radar, communications and jamming functionalities," *IEEE Trans. Wireless Commun.,* vol. 20, no. 1, pp. 83-95, Jan. 2021.

[13] S. Jin, W. Tan, M. Matthaiou, J. Wang, and K. Wong, "Statistical eigenmode transmission for the MU-MIMO downlink in Rician fading," *IEEE Trans. Wireless Commun.,* vol. 14, no. 12, pp. 6650-6663, Dec. 2015.

[14] X. Wang, H. Liang, and P. Wang, "Detection and tracking of UAVs using interferometric radar," in *2019 International Radar Conference (RADAR),* 2019, pp. 1-6.

[15] L. Liu, R. Zhang, and K. Chua, "Secrecy wireless information and power transfer with MISO beamforming," *IEEE Trans. Signal Process.,* vol. 62, no. 7, pp. 1850-1863, April1, 2014.

[16] T. P. Do and Y. H. Kim, "Resource allocation for a full-duplex wireless-powered communication network with imperfect self-interference cancelation," *IEEE Commun. Lett.,* vol. 20, no. 12, pp. 2482-2485, Dec. 2016.

[17] X. Wang, Z. Fei, J. Andrew Zhang, J. Huang, and J. Yuan, "Constrained utility maximization in dual-functional radar-communication multi-UAV networks," *IEEE Trans. Commun.,* vol. 69, no. 4, pp. 2660-2672, April 2021.

[18] P. Stoica, J. Li, and Y. Xie, "On probing signal design for MIMO radar," *IEEE Trans. Signal Process.,* vol. 55, no. 8, pp. 4151-4161, Aug. 2007.